Chapter 13
Strategies to Screen and to Identify New Genetic Loci Involved in the Regulation of Toxicity of Environmental Toxicants or Stresses

Abstract It is necessary to employ powerful strategies to screen and to identify new genetic loci involved in the regulation of toxicity of environmental toxicants or stresses in nematodes. We here introduced the usefulness of transcriptomic analysis, proteomic analysis, forward genetics, and reverse genetics in screening and in identifying new genetic loci involved in the regulation of toxicity of environmental toxicants or stresses. Meanwhile, we discussed the related limitations for these strategies in nematodes.

Keywords Transcriptomic analysis · Proteomic analysis · Forward genetics · Reverse genetics · Screen · *Caenorhabditis elegans*

13.1 Introduction

So far, most of the works on the elucidation of underlying molecular mechanisms for toxicity of environmental toxicants or stresses are relevant to those well-known signaling pathways. In nematode *Caenorhabditis elegans*, many environmental toxicants or stresses can potentially result in the toxicity at different aspects on animals [1–8]. Actually, during the toxicity induction of environmental toxicants or stresses, a complex network may exist and contain many relevant signaling pathways. Therefore, it is necessary to employ effective strategies to screen and to identify new genetic loci involved in the regulation of toxicity of environmental toxicants or stresses.

In this chapter, we first introduced the importance of transcriptomic analysis and proteomic analysis for the screen and the identification of new genetic loci involved in the regulation of toxicity of environmental toxicants or stresses. Moreover, we further introduced the importance of forward and reverse genetic screen techniques in screening and in identifying new genetic loci involved in the regulation of toxicity of environmental toxicants or stresses. The related advantages and limitations for these strategies were further discussed.

D. Wang, *Molecular Toxicology in Caenorhabditis elegans*,
https://doi.org/10.1007/978-981-13-3633-1_13

13.2 Transcriptomic Screen and Identification of New Genetic Loci Involved in the Regulation of Toxicity of Environmental Toxicants or Stresses

In nematodes, the transcriptomic technique has been widely and frequently employed to screen and to identify the new genetic loci involved in the regulation of toxicity of environmental toxicants or stresses [9–23]. The nanotoxicological studies have demonstrated that some of the engineered nanomaterials (ENMs) can potentially induce the toxic effects on the functions of both primary and secondary targeted organs in organisms, including the nematodes [24–30]. We here selected the multiwalled carbon nanotubes (MWCNTs), a carbon-based ENM, as an example to discuss the use of transcriptomic technique in screening and in identifying new genetic loci involved in the regulation of toxicity of environmental toxicants or stresses [31].

Using Illumina HiSeqTM 2000 sequencing technique, transcriptomes from both control and MWCNT exposure groups were sequenced to obtain clean read data after filtering raw sequence data containing adaptor fragments [31]. The analysis based on statistical significance and use of a 2.0-fold change cutoff was performed, and the acquired annotations of differentially expressed genes were compared with the databases of gene bank (Fig. 13.1) [31]. Among the detected 13,752 genes, totally, 1903 genes were differentially expressed in MWCNT-exposed nematodes compared with control (Fig. 13.1) [31]. Among these 1903 mRNAs, 924 mRNAs were upregulated, and 993 mRNAs were downregulated by MWCNT exposure [31]. Among these dysregulated genes, some genes were associated with the control of oxidative stress or intestinal development [31]. The dysregulated genes associated with the control of oxidative stress were *sod-2*, *sod-3*, *mev-1*, *isp-1*, *gas-1*, and *clk-1*, and the dysregulated genes associated with the control of intestinal development were *pgp-3*, *gem-4*, *par-3*, *pkc-3*, *ajm-1*, *lin-7*, *inx-3*, and *abts-4* [31].

To determine the biological processes mediated by the dysregulated genes in MWCNT-exposed nematodes, gene ontology analysis was performed. Based on the dysregulated mRNAs, the significantly influenced gene ontology terms could be mainly classified into several categories, which were at least associated with biological processes of development, reproduction, cell adhesion, apoptosis, enzyme activity, cellular component, cellular localization and transportation, response to stimulus, immune response, cell metabolism, macromolecular complex, transcription, and translation in organisms (Fig. 13.2) [31]. The KEGG pathway mapping, a bioinformatics resource used to map molecular data sets in genomics, was further

Fig. 13.1 (continued) expression levels are represented as blue, and relatively high expression levels are represented in red. (**b**) Scatter diagram of relationship between mRNA coverage of the control group and the MWCNT exposure group. (**c**) qRT-PCR analysis of the expressions of some genes encoding insulin signaling pathway in nematodes exposed to MWCNTs. (**d**) MWCNT exposure influenced the nuclear translocation of DAF-16::GFP in nematodes. Scale bar, 150 μm. MWCNT (1 mg/L) exposure was performed from L1-larvae to young adult. Bars represent means ± SEM $^{**}P < 0.01$ vs control

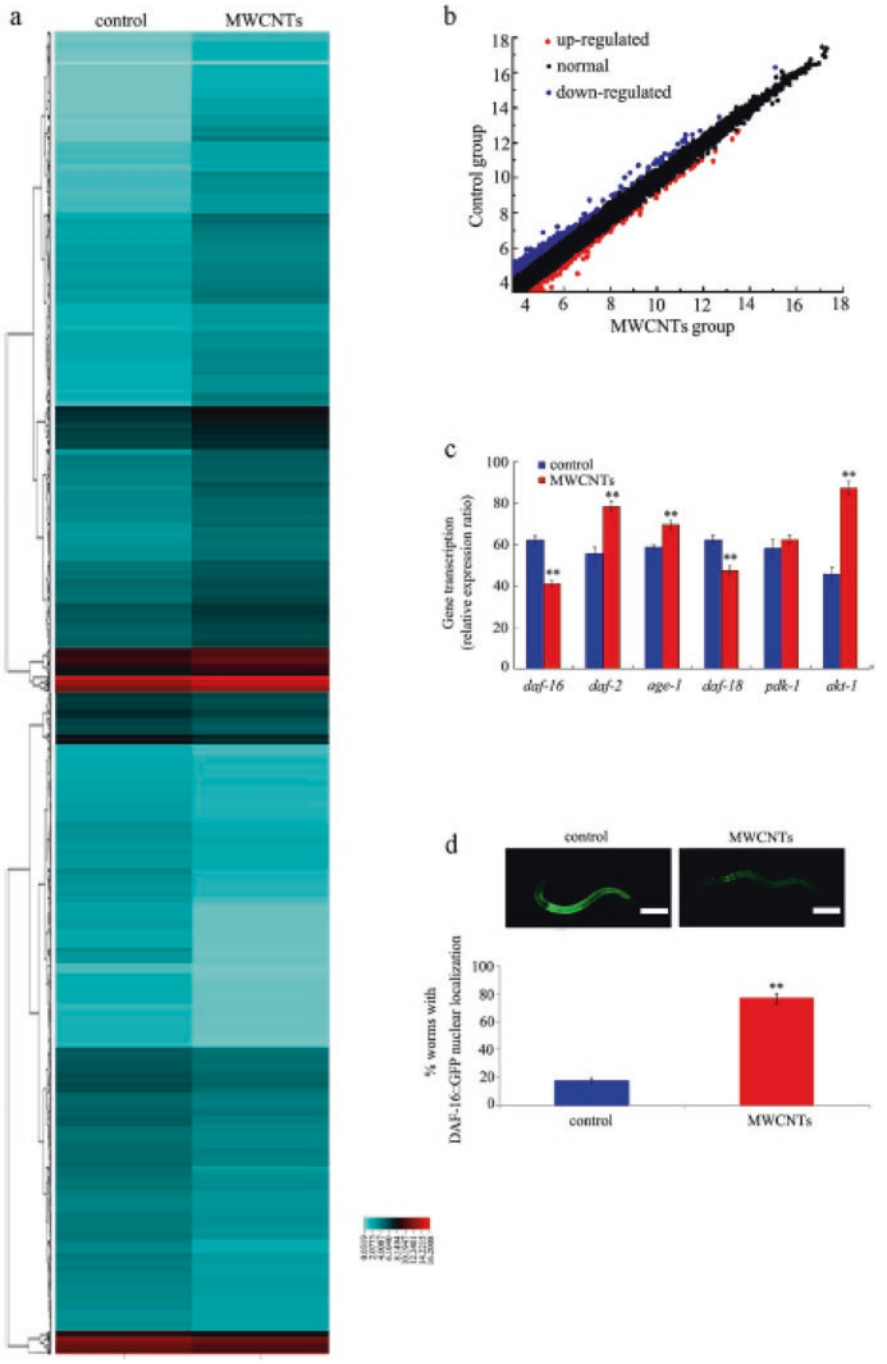

Fig. 13.1 Dysregulated mRNAs induced by MWCNT exposure [31]. (**a**) Heat map showing the expression of mRNAs obtained from control and MWCNT-exposed nematodes. Relatively low

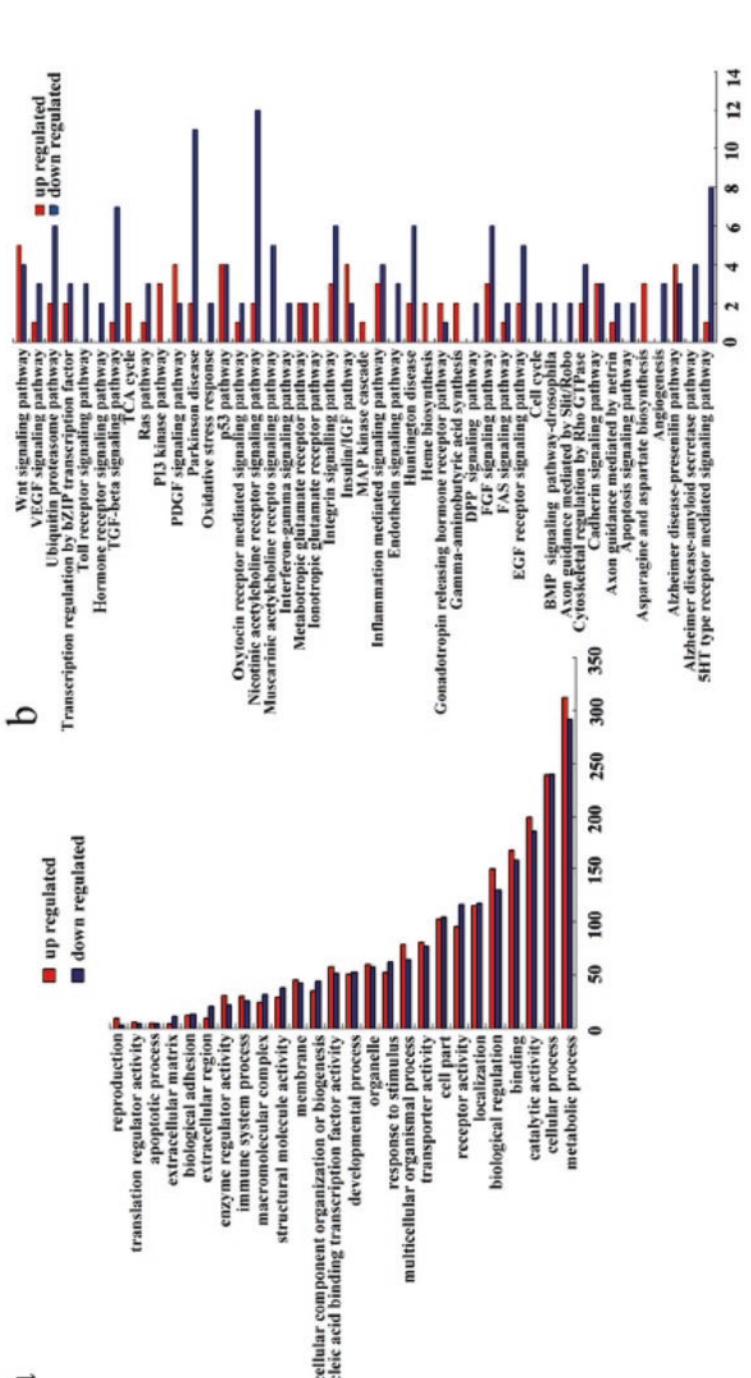

Fig. 13.2 Analysis of gene ontology terms and signaling pathways [31]. (**a**) Gene ontology terms with gene counts based on both down- and upregulated mRNAs in MWCNT-exposed nematodes. (**b**) Predicted KEGG signal pathways based on both down- and upregulated mRNAs in MWCNT-exposed nematodes

analyzed. The signaling pathways for the MWCNT toxicity control at least contained signaling pathways related to development, cell cycle, cell death, oxidative stress response, cellular component, immune response, neuronal development and neurodegeneration, and cell metabolism (Fig. 13.2) [31]. These results provide important clues for further understanding or elucidating the potential functions of dysregulated genes in the MWCNT toxicity induction in nematodes.

In nematodes, MWCNT exposure could induce the dysregulation of a series of miRNAs [32]. Among the dysregulated miRNAs, the bioinformatics analysis further demonstrated that *lin-4*, *mir-228*, *mir-249*, *mir-47*, *mir-355*, *mir-45*, *mir-2210*, *mir-57*, *mir-1018*, *mir-360*, *mir-64*, *mir-2209*, *mit-793*, *mir-1830*, *mir-2210*, *mir-83*, *mir-789*, and *mir-806* might be involved in the regulation of MWCNT toxicity through affecting the functions of identified dysregulated genes in exposed nematodes [31]. For example, *isp-1* gene might serve as a molecular target for *mir-249* to regulate the induction of oxidative stress in MWCNT-exposed nematodes [31]. Mutation of *mir-249* enhanced the induction of ROS production in MWCNT-exposed nematodes [31]. Mutation of *isp-1* inhibited the induction of ROS production in MWCNT-exposed nematodes, and mutation of *isp-1* gene suppressed the enhanced induction of ROS production observed in MWCNT-exposed *mir-249(n4983)* mutant nematodes [31]. The raised miRNA–mRNA network provides another important clue for the further elucidation of underlying molecular mechanisms of MWCNT toxicity induction in nematodes.

In nematodes, the insulin signaling pathway plays a crucial role in the regulation of toxicity of environmental toxicants or stresses [1, 33–35]. Among the genes encoding the insulin signaling pathway, the transcriptional expressions of *daf-16* and *daf-18* were decreased, and the transcriptional expressions of *age-1*, *daf-2*, *pdk-1*, and *akt-1* were increased in MWCNT (1 mg/L)-exposed nematodes compared with control (Fig. 13.1) [31]. The qRT-PCR assay confirmed these changes (Fig. 13.1) [31]. *daf-2* encodes a protein that is homologous to human insulin receptor InR, *age-1* encodes a protein that is homologous to human phosphoinositide 3-kinase PI3K, *daf-18* encodes a protein that is homologous to human lipid phosphatase PTEN, *akt-1* encodes a protein that is homologous to human serine/threonine kinase Akt/PKB, and *daf-16* encodes a protein that is homologous to human transcription factor FOXO. Meanwhile, it was observed that the percentage of nematodes with DAF-16::GFP in nucleus was significantly increased compared with control after the exposure to MWCNTs (Fig. 13.1) [31].

Moreover, it was found that mutation of *daf-2*, *age-1*, or *akt-1* led to the obvious inhibition in induction of ROS production in the intestine and the significant increase in brood size or locomotion behavior in MWCNT (1 mg/L)-exposed nematodes; however, mutation of *daf-16* or *daf-18* resulted in the enhanced induction of ROS production in the intestine and the more severe decrease in brood size or locomotion behavior in MWCNT (1 mg/L)-exposed nematodes (Fig. 13.3) [31]. Therefore, the functional analysis demonstrated the crucial role of the insulin signaling pathway in regulating the MWCNT toxicity in nematodes.

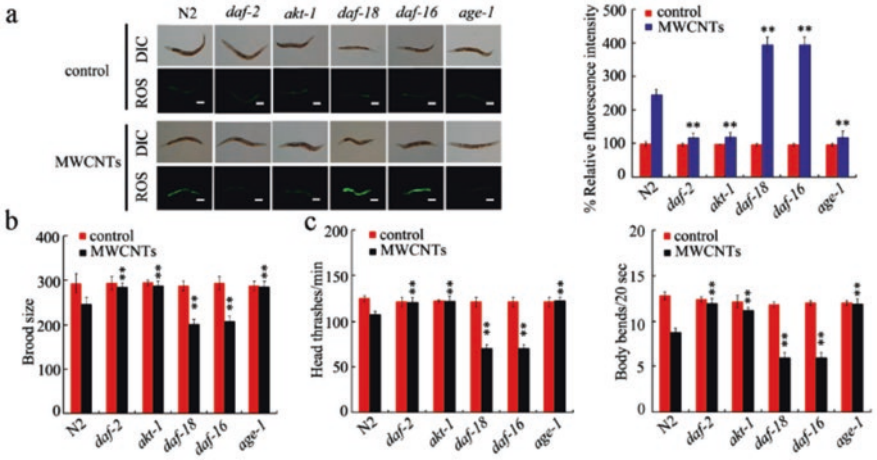

Fig. 13.3 Genes encoding insulin signaling pathway were involved in the control of MWCNT toxicity in nematodes [31]. (**a**) Intestinal ROS production assay in mutants for genes encoding insulin signaling pathway. Scale bar, 150 μm. (**b**) Brood size assay in mutants for genes encoding insulin signaling pathway. (**c**) Locomotion behavior assay in mutants for genes encoding insulin signaling pathway. Locomotion behavior was assessed by the endpoints of head thrash and body bend. The used nematode strains were wild-type N2, *daf-16(mu86)*, *daf-2(e1370)*, *age-1(hx546)*, *daf-18(e1375)*, and *akt-1(ok525)*. MWCNT (1 mg/L) exposure was performed from L1-larvae to young adult. Bars represent means ± SEM $^{**}P < 0.01$ vs N2

13.3 Proteomic Screen and Identification of New Genetic Loci Involved in the Regulation of Toxicity of Environmental Toxicants or Stresses

With the acrylamide as an example, the second-dimension SDS-PAGE was performed to analyze the differences in protein expressions in acrylamide-exposed nematodes. Totally 274 ± 31 spots from the control extracts and 334 ± 29 spots from acrylamide (500 mg/l)-treated extracts were detected (Fig. 13.4) [36]. Among these spots, 14 spots were identified as dysregulated spots by MALDI-TOF mass spectrometer (Fig. 13.4) [36]. Moreover, four proteins were clearly upregulated by 500 mg/l of acrylamide, and these were all GSTs [36].

It was further observed that the GST expressions were induced by acrylamide (500 mg/l) exposure for 12, 24, and 48 h (Fig. 13.5) [36]. Especially, the obvious alteration in expressions of GST-4, GST-7, GST-38, and GST-30 could be induced by acrylamide (500 mg/l) [36]. After acrylamide (500 mg) exposure for 48 h, the GST-4 expression was strongest, and RNAi knockdown of *skn-1* suppressed this expression induction in the pharynx and in the body wall muscle [36].

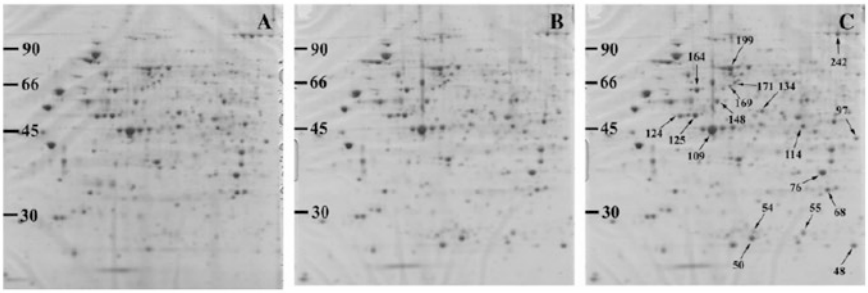

Fig. 13.4 2-DE gel images of *Caenorhabditis elegans* total protein [36]. Five hundred microgram of protein was separated in the first dimension by pH gradient (pH 4–7, 18 cm) and in the second dimension by molecular weight. (**a**) Proteins from animals grown on control plates without acrylamide; 277 ± 31 (mean ± SD) protein spots were detected from four independent experiments. (**b**) Proteins from animals grown on 500 mg/l acrylamide; 334 ± 29 (mean ± SD) protein spots were detected from four independent experiments. (**c**) Eighteen identified spots are indicated on a 2-DE gel image

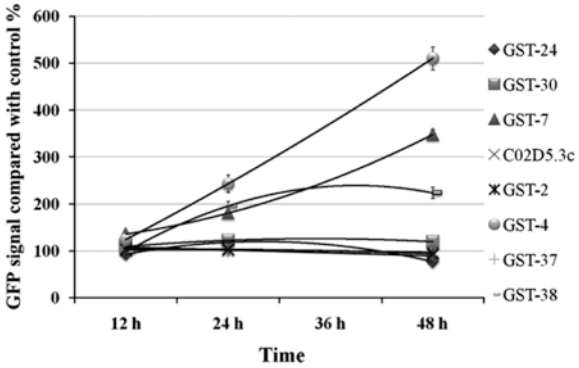

Fig. 13.5 Changes in the GST expression of the eight transgenic animals exposed from the L1 stage to 500 mg/l of acrylamide for 12, 24, and 48 h [36]. Animals were alive after all measurements. Data points indicate mean values ± SEM of three independent experiments. Statistical significance was shown by the GFP signals from 12 h for GST-4, GST-7, and GST-30 and from 24 h for GST-38 ($p < 0.05$)

13.4 Forward Genetic Screen and Identification of New Genetic Loci Involved in the Regulation of Toxicity of Environmental Toxicants or Stresses

The forward genetic screen is a powerful genetic tool to identify new genetic loci involved in the regulation of toxicity of environmental toxicants or stresses in nematodes [37, 38]. In nematodes, the excess iodide caused pleiotropic defects on animals [39]. We here selected the iodide toxicity as an example to introduce the use of

forward genetics for the screen and the identification of new genetic loci involved in the regulation of toxicity of environmental toxicants or stresses.

The P0 nematodes were mutagenized with ethyl methanesulfonate, and the phenotypes were screened in 5000 F1 animals [39]. The mutants that could survive in 5 mM NaI were saved, and 12 independent isolates were obtained [39]. After mapping using SNPs and genetic complementation tests of all 12 mutations, these mutations might affect at least 4 genes [39].

Using nuclear-binding fluorescence dye Hoechst 33258, five isolates (*mac33*, *mac38*, *mac40*, *mac42*, and *mac43*) exhibited a defective cuticle integrity (Fig. 13.6) [39], suggesting the genetic lesions affecting cuticle formation. In nematodes, mutations affecting cuticles usually cause blisters on cuticle (Bli), dumpy (Dpy), long (Lon), roller (Rol), and/or squat (Sqt). Because only an obviously Bli phenotype

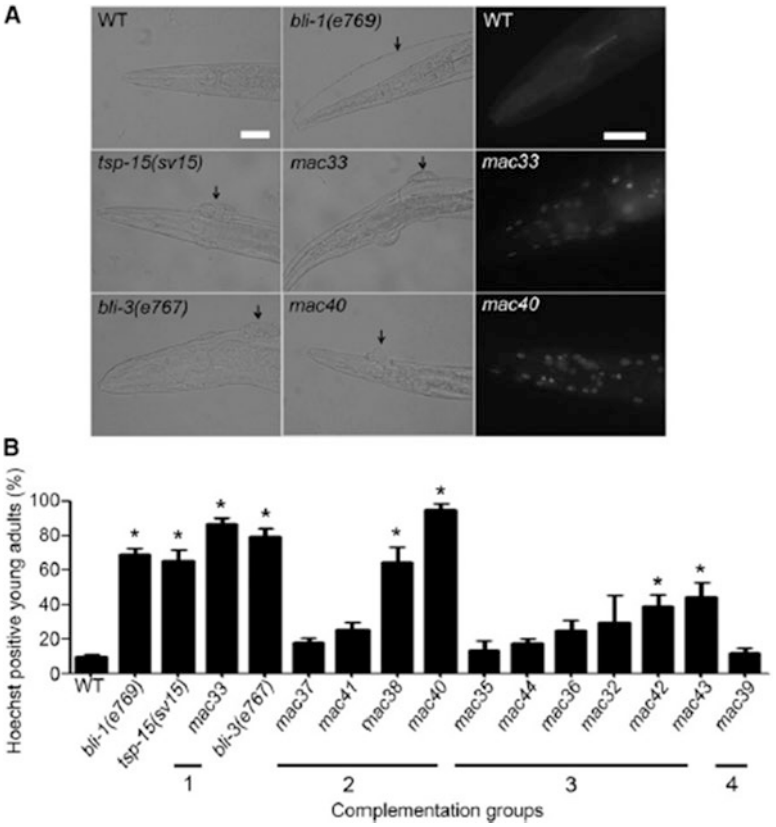

Fig. 13.6 Mutants that survive in 5 mM NaI have defective cuticle integrity [39]. (**a**) Cuticle blisters (arrows) of *bli* mutants, *tsp-15(sv15)* mutants, and two *mac* mutants (left and middle panels). Hoechst 33258 labels numerous nuclei in *mac33* and *mac40* mutants (right panels). Scale bars, 20 mm. (**b**) Ratios of Hoechst 33258-positive animals. Statistics, different from wild type. Bars, SEs of four biological replicates ($n = 50$ for each replicate). $^{*}P < 0.01$ (Bonferroni test with one-way ANOVA)

was detected in *mac* isolates, it was postulated that the Bli mutants might potentially survive in excess iodide [39]. Nevertheless, the further test on a series of Bli mutants (*bli-1(e769)*, *bli-2(e768)*, *bli-3(e767)*, *bli-4(e937)*, *bli-5(e518)*, *bli-6(n776*, *sc16)*, and *tsp-15(sv15)*) indicated that only *bli-3*(*e767*) and *tsp-15*(*sv15*) mutant nematodes could survive in the excess iodide [39].

It was found that three of four complementation groups were mapped to chromosome I, on which both *bli-3* and *tsp-15* locate [39]. Moreover, *mac40* is an allele of *bli-3*, *mac33* is an allele of *tsp-15*, and *mac32* represents an unknown gene (Fig. 13.7) [39]. Meanwhile, the blisters of *mac33* and *mac40* mutant nematodes resemble those of *tsp-15*(*sv15*) and *bli-3(e767)* mutant nematodes but are still different from the clear blisters of *bli-1*(*e769*) mutants (Fig. 13.7) [39]. Additionally, nematodes with RNAi knockdown of *bli-3* or *tsp-15* could survive in 5 mM NaI [39].

In nematodes, the DOXA-1, an ortholog of mammalian dual oxidase maturation factor, forms a complex with BLI-3 and TSP-15, and each component of BLI-3/TSP-15/DOXA-1 dual oxidase complex was found to be required for the development-arresting effect of excess iodide [39]. The nematodes with RNAi knockdown of *mtl-7* encoding a ShkT (Shk toxin)-domain-containing heme peroxidase were Bli but failed to survive in 5 mM NaI [39]. Meanwhile, RNAi knockdown of *mlt-7* and each *skpo* gene (*skpo-1*, *skpo-2*, or *skpo-3*) encoding other

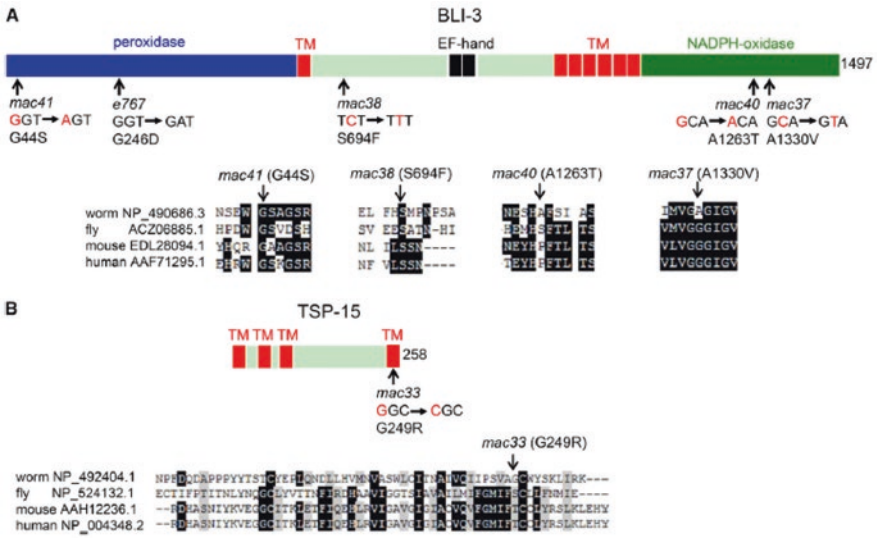

Fig. 13.7 Some *mac* mutations affect *bli-3* and *tsp-15* [39]. (**a**) The *mac* mutations in *bli-3* affect conserved (*mac41*, G44S; *mac38*, S694F) or nonconserved (*mac40*, A1263T; *mac37*, A1330V) amino acids in different domains of BLI-3. Nucleotide changes, amino acid changes, and BLI-3 DUOX1 partial sequence alignments of different species were presented. TM, transmembrane domain. (**b**) *mac33* affects a nonconserved amino acid residue in the fourth transmembrane domain of TSP-15. Nucleotide change, amino acid change, and TSP-15 partial sequence alignment were presented

ShkT-domain-containing peroxidases individually or in combination did not result in the survival phenotype in excess iodide [39], suggesting that MLT-7 and each of the SKPO proteins might not be redundantly required for development-arresting effect in response to the excess iodide.

13.5 Reverse Genetic Screen and Identification of New Genetic Loci Involved in the Regulation of Toxicity of Environmental Toxicants or Stresses

13.5.1 Using a Certain Number of Mutants to Screen and to Identify Genetic Loci Involved in the Regulation of Toxicity of Environmental Toxicants or Stresses

The mutant resources for nematodes are very rich, and thus, using a certain number of mutants is frequently employed to screen and to identify genetic loci involved in the regulation of toxicity of environmental toxicants or stresses [40–42]. Environmental pathogens can potentially cause the toxicity or even kill the host organisms, including the nematodes [43–50]. We here further select the pathogen infection as an example to introduce the use of mutants to screen and to identify microRNAs (miRNAs) involved in the regulation of toxicity of environmental toxicants or stresses in nematodes [51].

Using deletion mutants, a large-scale screen was performed to identify the miRNAs involved in the control of *P. aeruginosa* PA14 infection and the corresponding innate immune response [51]. Based on the phenotypic analysis of survival in miRNA mutants infected with *P. aeruginosa* PA14, totally 11 out of the examined 82 miRNA mutants with the abnormal survival phenotype were identified (Fig. 13.8) [51]. These miRNA mutants were *let-7(mg279)*, *mir-45(n4280)*, *mir-63(n4568)*, *mir-75(n4472)*, *mir-84(n4307)*, *mir-233(n4761)*, *mir-241(n4316)*, *mir-246(n4636)*, *mir-256(n4471)*, *mir-355(n4618)*, and *mir-360(n4635)* (Fig. 13.8) [51]. Loss-of-function mutation of *let-7*, *mir-45*, *mir-75*, *mir-84*, *mir-241*, *mir-246*, or *mir-256* caused a resistance to *P. aeruginosa* PA14 infection in reducing survival (Fig. 13.8) [51]. In contrast, loss-of-function mutation of *mir-63*, *mir-233*, *mir-360*, or *mir-355* resulted in a susceptibility to *P. aeruginosa* PA14 infection in reducing survival (Fig. 13.8) [51].

Colony-forming unit (CFU) was employed to determine the PA14 colony formation in the body of miRNA mutant after *P. aeruginosa* infection. After *P. aeruginosa* PA14 infection, loss-of-function mutation of *mir-63*, *mir-360*, or *mir-355* enhanced the PA14 colony formation in the body of nematodes; however, loss-of-function mutation of *mir-45*, *mir-75*, *mir-246*, or *mir-256* suppressed the PA14 colony formation in the body of nematodes (Fig. 13.9) [51].

P. aeruginosa PA14 infection can increase the transcriptional expression of antimicrobial genes. Some putative antimicrobial genes (*lys-1*, *lys-8*, *clec-85*, *dod-22*,

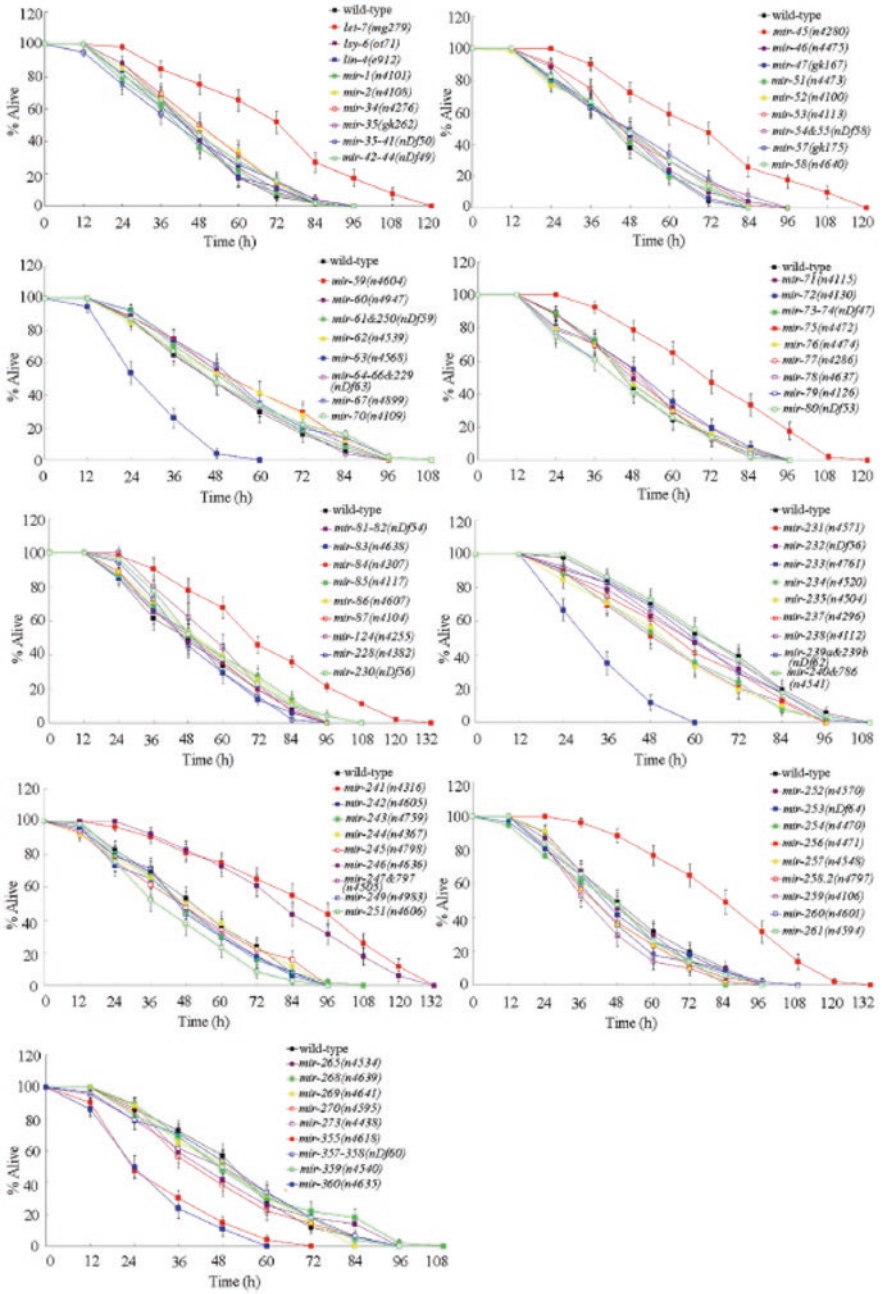

Fig. 13.8 Survival in miRNA mutants infected with *P. aeruginosa* PA14 [51]. Bars represent mean ± SD

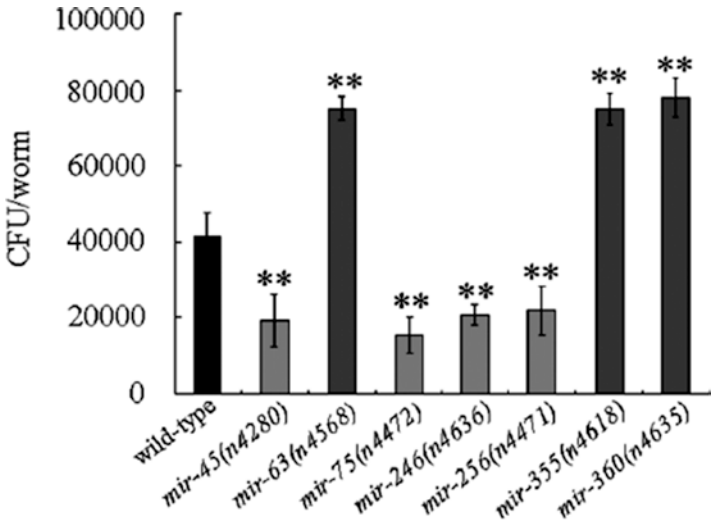

Fig. 13.9 *P. aeruginosa* PA14 CFU in the body of miRNA mutants infected with *P. aeruginosa* PA14 [51]. Bars represent mean ± SD. $^{**}P < 0.01$ vs wild type

K08D8.5, *F55G11.7*, and *F55G11.4*) were selected to determine the innate immune response in *P. aeruginosa* PA14 infected miRNA mutants. *lys-1* and *lys-8* encode lysozymes, *clec-85* encodes a C-type lectin protein, *dod-22* and *F55G11.7* encode orthologs of human epoxide hydrolase 1, and *K08D8.5* and *F55G11.4* encode CUB-like domain-containing proteins. After *P. aeruginosa* PA14 infection, mutation of *mir-45* increased the expressions of *lys-8*, *clec-85*, *dod-22*, *F55G11.7*, and *F55G11.4*; mutation of *mir-75* increased the expressions of *lys-1*, *lys-8*, *dod-22*, *F55G11.7*, and *F55G11.4*; mutation of *mir-246* increased the expressions of *lys-8*, *clec-85*, *dod-22*, *K08D8.5*, and *F55G11.7*; and mutation of *mir-256* increased the expressions of *lys-1*, *lys-8*, *clec-85*, *dod-22*, and *K08D8.5* (Fig. 13.10) [51]. Different from these, mutation of *mir-63* decreased the expressions of *lys-1*, *dod-22*, *F55G11.7*, and *F55G11.4*; mutation of *mir-355* decreased the expressions of *lys-1*, *lys-8*, *K08D8.5*, *F55G11.7*, and *F55G11.4*; and mutation of *mir-360* decreased the expressions of *lys-8*, *dod-22*, *K08D8.5*, and *F55G11.7* (Fig. 13.10) [51]. These results suggest that loss-of-function mutation of these seven miRNAs alters the innate immune response of nematodes to *P. aeruginosa* PA14 infection in nematodes.

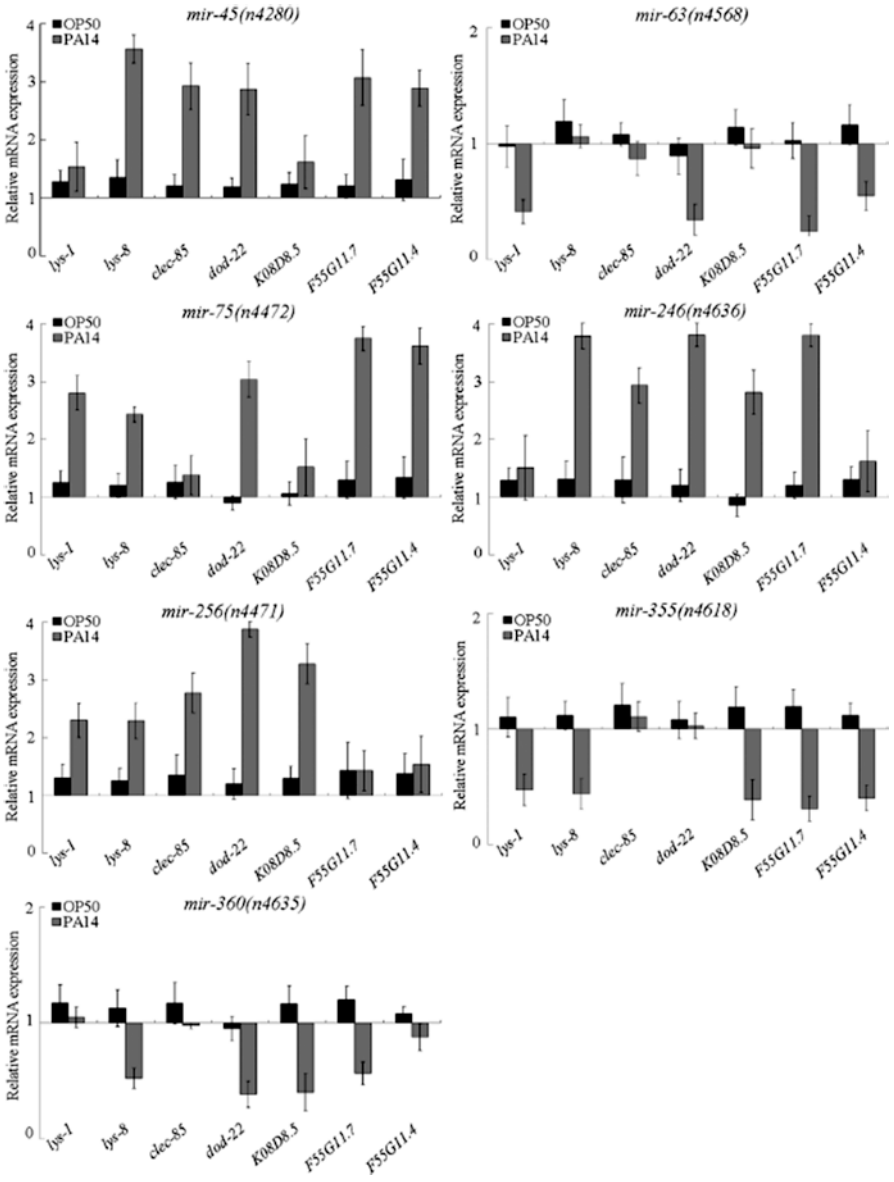

Fig. 13.10 Expression patterns of putative antimicrobial genes in *P. aeruginosa* PA14 infected miRNA mutant nematodes [51]. Normalized expression is presented relative to wild-type expression. Bars represent mean ± SD

13.5.2 Using RNAi Knockdown Technique to Screen and to Identify Genetic Loci Involved in the Regulation of Toxicity of Environmental Toxicants or Stresses

Myotonic dystrophy disorders can be induced by expanded CUG repeats in noncoding regions. The reporter constructs without any CUG repeats in the 384-nt 3′ UTR from *let-858* (0CUG) showed a strong GFP fluorescence, whereas the presence of 123 CUG repeats in the 3′ UTR (123CUG) resulted in a sharp decline in GFP fluorescence [52]. Using the decline in adult-stage GFP fluorescence in 123CUG transgenic nematodes, RNAi screen was performed to identify the gene inactivations that can modify toxicity of expanded-CUG-repeat RNA [52]. After an initial fluorescence-based RNAi screen, a secondary motility-based screen of hits from the primary screen was further performed [52]. An RNAi library of 403 clones targeting genes that encode RNA-binding proteins and factors implicated in small-RNA pathways was screened. After the rescreening in triplicate, 84 gene inactivations were observed to induce an increase in late-developmental-stage GFP fluorescence in the 123CUG strain without affecting the control 0CUG strain (Fig. 13.11) [52]. Among these genes, 14 gene inactivations could further significantly increase or decrease the velocity of 123CUG animals without affecting the control (0CUG) animals (Fig. 13.11) [52].

13.6 Perspectives

No doubt, all the four introduced strategies in this chapter are powerful and effective for the screen and the identification of new genetic loci involved in the regulation of toxicity of environmental toxicants or stresses. Nevertheless, meanwhile, these strategies have certain limitations.

With the concern on the transcriptomic analysis, it has at least two aspects of limitations. Firstly, this strategy cannot reflect the alterations at the translational level. Secondly, this strategy itself cannot tell us the biological or toxicological function of candidate genes. Nevertheless, this strategy can provide us a large number of candidate genes for further consideration.

With the concern on the proteomic analysis, it has also at least two aspects of limitations. Firstly, largely due to the 2-D SDS-PAGE technical limitation, usually only very limited dysregulated proteins can be identified. Secondly, data from this strategy still need the further functional analysis and confirmation.

With the concern on the forward genetics, these two aspects should be paid attention to. On the one hand, the number of obtained candidate mutants is usually largely affected by the examined phenotype or endpoint. The subtle phenotype or sensitive endpoint may be helpful for us to obtain more candidate mutants. On the other hand, this strategy still needs the further examination on the expression of candidate genes corresponding to the obtained mutants in nematodes exposed to

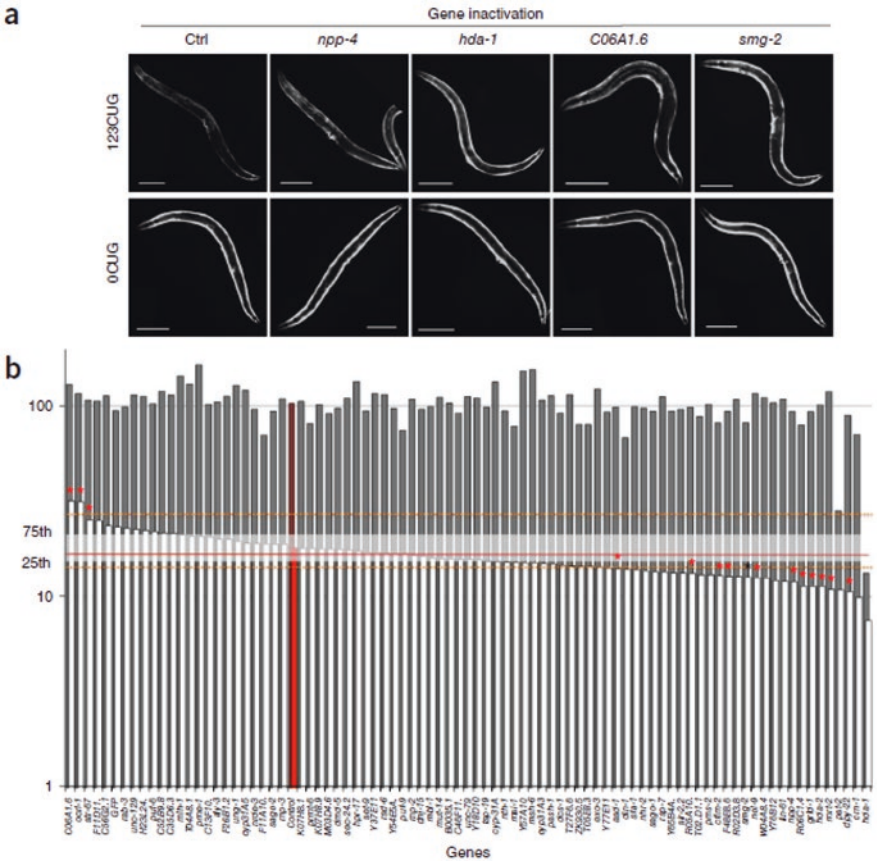

Fig. 13.11 Identification of gene inactivations that modulate expanded-CUG-repeat toxicity [52]. (**a**) Gene inactivations that disrupt the late-stage downregulation of GFP fluorescence mediated by 123CUG in the 3′ UTR. Fluorescence microscopy images of the strains 123CUG and the control 0CUG, on different RNAi gene inactivations: empty vector control (ctrl), *npp-4*, *hda-1*, *C06A1.6*, and *smg-2*. Images were taken at the 3-day-old adult stage. Bar, 200 µm. (**b**) Genetic suppressors and enhancers of expanded-CUG-repeat toxicity. Graph of velocity measurements of 0CUG (gray) and 123CUG (white) animals fed on different gene inactivations. The plotted velocities (x-axis, in µm/s) correspond to the median values of three independent experiments for *aly-3*, *asd-1*, *C52B9.8*, *C06A1.6*, *cfim-2*, *dpy-2*, *F26B1.2*, *F48E8.6*, *grld-1*, *hda-1*, *hda-2*, *mrt-2*, *msh-6*, *nhr-2*, *nol-9*, *nth-1*, *pst-2*, *puf-6*, *puf-9*, *R05D10.1*, *R06C1.4*, *rnp-3*, sago-1, sec-24.2, sfa-1, sir-2.2, *smg-2*, *str-67*, *ung-1*, and *Y65B4A1* of 2 experiments for all other tested genes and of 22 experiments for control L4440. Red bars, strains fed on control vector; red line, median velocity; white shading, 25th and 75th percentiles, as indicated, for the 123CUG animals fed on control vector; dotted orange lines, maximum (upper) and minimum (lower) of the median velocity for 123CUG animals fed on control vector; and red asterisks, significant gene inactivations, as determined by Kolmogorov–Smirnov *P* value. The number of animals analyzed varied from 50 to 250 animals depending on the RNAi clone (further described in Online Methods), with a total of 1384 animals analyzed for the L4440 control. The black asterisk indicates the gene *smg-2*

environmental toxicants or stresses. The important advantage for this strategy is to be able to obtain the mutants with the anticipated phenotypes.

With the concern on the reverse genetics, it has at least two aspects of limitations. Firstly, this strategy also needs the further examination on the expression of candidate genes corresponding to the obtained mutants in nematodes exposed to environmental toxicants or stresses. Secondly, the powerfulness of this strategy to identify new genetic loci involved in the regulation of toxicity of environmental toxicants or stresses is somewhat limited. Usually, for the screened mutants, the functions of corresponding genes are already known. That is, for this strategy, a large-scale screen is suggested.

Taken together, to screen and to identify new genetic loci involved in the regulation of toxicity of environmental toxicants or stresses, we should consider both of these two aspects simultaneously. On the one hand, we hope to be able to identify candidate genetic loci with the functions in regulating the toxicity of environmental toxicants or stresses. On the other hand, we need to carefully examine the alterations in expression of these candidate genetic loci in nematodes exposed to environmental toxicants or stresses. Lacking any one aspect is not reasonable for the elucidation of underlying molecular mechanisms for the observed toxicity induced by certain environmental toxicants or stresses in nematodes.

References

1. Wang D-Y (2018) Nanotoxicology in *Caenorhabditis elegans*. Springer, Singapore
2. Qu M, Xu K-N, Li Y-H, Wong G, Wang D-Y (2018) Using *acs-22* mutant *Caenorhabditis elegans* to detect the toxicity of nanopolystyrene particles. Sci Total Environ 643:119–126
3. Dong S-S, Qu M, Rui Q, Wang D-Y (2018) Combinational effect of titanium dioxide nanoparticles and nanopolystyrene particles at environmentally relevant concentrations on nematodes *Caenorhabditis elegans*. Ecotoxicol Environ Saf 161:444–450
4. Li W-J, Wang D-Y, Wang D-Y (2018) Regulation of the response of *Caenorhabditis elegans* to simulated microgravity by p38 mitogen-activated protein kinase signaling. Sci Rep 8:857
5. Xiao G-S, Zhao L, Huang Q, Yang J-N, Du H-H, Guo D-Q, Xia M-X, Li G-M, Chen Z-X, Wang D-Y (2018) Toxicity evaluation of Wanzhou watershed of Yangtze Three Gorges Reservoir in the flood season in *Caenorhabditis elegans*. Sci Rep 8:6734
6. Xiao G-S, Zhao L, Huang Q, Du H-H, Guo D-Q, Xia M-X, Li G-M, Chen Z-X, Wang D-Y (2018) Biosafety assessment of water samples from Wanzhou watershed of Yangtze Three Gorges Reservoir in the quiet season in *Caenorhabditis elegans*. Sci Rep 8:14102
7. Yin J-C, Liu R, Jian Z-H, Yang D, Pu Y-P, Yin L-H, Wang D-Y (2018) Di (2-ethylhexyl) phthalate-induced reproductive toxicity involved in DNA damage-dependent oocyte apoptosis and oxidative stress in *Caenorhabditis elegans*. Ecotoxicol Environ Saf 163:298–306
8. Wu Q-L, Han X-X, Wang D, Zhao F, Wang D-Y (2017) Coal combustion related fine particulate matter ($PM_{2.5}$) induces toxicity in *Caenorhabditis elegans* by dysregulating microRNA expression. Toxicol Res 6:432–441
9. Starnes DL, Lichtenberg SS, Unrine JM, Starnes CP, Oostveen EK, Lowry GV, Bertsch PM, Tsyusko OV (2016) Distinct transcriptomic responses of *Caenorhabditis elegans* to pristine and sulfidized silver nanoparticles. Environ Pollut 213:314–321

10. Lewis JA, Gehman EA, Baer CE, Jackson DA (2013) Alterations in gene expression in *Caenorhabditis elegans* associated with organophosphate pesticide intoxication and recovery. BMC Genomics 14:291
11. McElwee MK, Ho LA, Chou JW, Smith MV, Freedman JH (2013) Comparative toxicogenomic responses of mercuric and methyl-mercury. BMC Genomics 14:698
12. Chatterjee N, Kim Y, Yang J, Roca CP, Joo S, Choi J (2016) A systems toxicology approach reveals the Wnt-MAPK crosstalk pathway mediated reproductive failure in *Caenorhabditis elegans* exposed to graphene oxide (GO) but not to reduced graphene oxide (rGO). Nanotoxicology 11:76–86
13. Menzel R, Yeo HL, Rienau S, Li S, Steinberg CEW, Stürzenbaum SR (2007) Cytochrome P450s and short-chain dehydrogenases mediate the toxicogenomic response of PCB52 in the nematode *Caenorhabditis elegans*. J Mol Biol 370:1–13
14. Lewis JA, Szilagyi M, Gehman E, Dennis WE, Jackson DA (2009) Distinct patterns of gene and protein expression elicited by organophosphorus pesticides in *Caenorhabditis elegans*. BMC Genomics 10:202
15. Roh J, Sim SJ, Yi J, Park K, Chung KH, Ryu D, Choi J (2009) Ecotoxicity of silver nanoparticles on the soil nematode *Caenorhabditis elegans* using functional ecotoxicogenomics. Environ Sci Technol 43:3933–3940
16. Eom H, Kim H, Kim B, Chon T, Choi J (2014) Integrative assessment of benzene exposure to *Caenorhabditis elegans* using computational behavior and toxicogenomic analyses. Environ Sci Technol 48:8143–8151
17. Menzel R, Swain SC, Hoess S, Claus E, Menzel S, Steinberg CEW, Reifferscheid G, Stürzenbaum SR (2009) Gene expression profiling to characterize sediment toxicity – a pilot study using *Caenorhabditis elegans* whole genome microarrays. BMC Genomics 10:160
18. Vin uela A, Snoek LB, Riksen JAG, Kammenga JE (2010) Genome-wide gene expression analysis in response to organophosphorus pesticide chlorpyrifos and diazinon in *C. elegans*. PLoS ONE e12145:5
19. Sahu SN, Lewis J, Patel I, Bozdag S, Lee JH, Sprando R, Cinar HN (2013) Genomic analysis of stress response against arsenic in *Caenorhabditis elegans*. PLoS ONE 8:e66431
20. Boehler CJ, Raines AM, Sunde RA (2014) Toxic-selenium and low-selenium transcriptomes in *Caenorhabditis elegans*: toxic selenium up-regulates oxidoreductase and down-regulates cuticle-associated genes. PLoS ONE 9:e101408
21. Rudgalvyte M, VanDuyn N, Aarnio V, Heikkinen L, Peltonen J, Lakso M, Nass R, Wong G (2013) Methylmercury exposure increases lipocalin related (*lpr*) and decreases activated in blocked unfolded protein response (*abu*) genes and specific miRNAs in *Caenorhabditis elegans*. Toxicol Lett 222:189–196
22. Cui Y, McBride SJ, Boyd WA, Alper S, Freedman JH (2007) Toxicogenomic analysis of *Caenorhabditis elegans* reveals novel genes and pathways involved in the resistance to cadmium toxicity. Genome Biol 8:R122
23. Tsyusko OV, Unrine JM, Spurgeon D, Blalock E, Starnes D, Tseng M, Joice G, Bertsch PM (2012) Toxicogenomic responses of the model organism *Caenorhabditis elegans* to gold nanoparticles. Environ Sci Technol 46:4115–4124
24. Ren M-X, Zhao L, Ding X-C, Krasteva N, Rui Q, Wang D-Y (2018) Developmental basis for intestinal barrier against the toxicity of graphene oxide. Part Fibre Toxicol 15:26
25. Xiao G-S, Chen H, Krasteva N, Liu Q-Z, Wang D-Y (2018) Identification of interneurons required for the aversive response of *Caenorhabditis elegans* to graphene oxide. J Nanobiotechnol 16:45
26. Ding X-C, Rui Q, Wang D-Y (2018) Functional disruption in epidermal barrier enhances toxicity and accumulation of graphene oxide. Ecotoxicol Environ Saf 163:456–464
27. Zhao L, Kong J-T, Krasteva N, Wang D-Y (2018) Deficit in epidermal barrier induces toxicity and translocation of PEG modified graphene oxide in nematodes. Toxicol Res 7(6):1061–1070. https://doi.org/10.1039/C8TX00136G

28. Shao H-M, Han Z-Y, Krasteva N, Wang D-Y (2018) Identification of signaling cascade in the insulin signaling pathway in response to nanopolystyrene particles. Nanotoxicology in press
29. Xiao G-S, Zhi L-T, Ding X-C, Rui Q, Wang D-Y (2017) Value of *mir-247* in warning graphene oxide toxicity in nematode *Caenorhabditis elegans*. RSC Adv 7:52694–52701
30. Wang Q-Q, Zhao S-Q, Zhao Y-L, Rui Q, Wang D-Y (2014) Toxicity and translocation of graphene oxide in *Arabidopsis* plants under stress conditions. RSC Adv 4:60891–60901
31. Zhao Y-L, Yang J-N, Wang D-Y (2016) A microRNA-mediated insulin signaling pathway regulates the toxicity of multi-walled carbon nanotubes in nematode *Caenorhabditis elegans*. Sci Rep 6:23234
32. Zhao Y-L, Wu Q-L, Li Y-P, Nouara A, Jia R-H, Wang D-Y (2014) In vivo translocation and toxicity of multi-walled carbon nanotubes are regulated by microRNAs. Nanoscale 6:4275–4284
33. Ren M-X, Zhao L, Lv X, Wang D-Y (2017) Antimicrobial proteins in the response to graphene oxide in *Caenorhabditis elegans*. Nanotoxicology 11:578–590
34. Zhuang Z-H, Li M, Liu H, Luo L-B, Gu W-D, Wu Q-L, Wang D-Y (2016) Function of RSKS-1-AAK-2-DAF-16 signaling cascade in enhancing toxicity of multi-walled carbon nanotubes can be suppressed by *mir-259* activation in *Caenorhabditis elegans*. Sci Rep 6:32409
35. Zhao Y-L, Yang R-L, Rui Q, Wang D-Y (2016) Intestinal insulin signaling encodes two different molecular mechanisms for the shortened longevity induced by graphene oxide in *Caenorhabditis elegans*. Sci Rep 6:24024
36. Hasegawa K, Miwa S, Isomura K, Tsutsumiuchi K, Taniguchi H, Miwa J (2008) Acrylamide-responsive genes in the nematode *Caenorhabditis elegans*. Toxicol Sci 101:215–225
37. Bruinsma JJ, Schneider DL, Davis DE, Kornfeld K (2008) Identification of mutations in *Caenorhabditis elegans* that cause resistance to high levels of dietary zinc and analysis using a genomewide map of single nucleotide polymorphisms scored by pyrosequencing. Genetics 179:811–828
38. Munoz MJ, Riddle DL (2003) Positive selection of *Caenorhabditis elegans* mutants with increased stress resistance and longevity. Genetics 163:171–180
39. Xu Z, Luo J, Li Y, Ma L (2015) The BLI-3/TSP-15/DOXA-1 dual oxidase complex is required for iodide toxicity in *Caenorhabditis elegans*. G3 5:195–203
40. Rui Q, Zhao Y-L, Wu Q-L, Tang M, Wang D-Y (2013) Biosafety assessment of titanium dioxide nanoparticles in acutely exposed nematode *Caenorhabditis elegans* with mutations of genes required for oxidative stress or stress response. Chemosphere 93:2289–2296
41. Ahn J, Eom H, Yang X, Meyer JN, Choi J (2014) Comparative toxicity of silver nanoparticles on oxidative stress and DNA damage in the nematode, *Caenorhabditis elegans*. Chemosphere 108:343–352
42. Wu Q-L, Zhao Y-L, Li Y-P, Wang D-Y (2014) Susceptible genes regulate the adverse effects of TiO_2-NPs at predicted environmental relevant concentrations on nematode *Caenorhabditis elegans*. Nanomedicine 10:1263–1271
43. Wu Q-L, Cao X-O, Yan D, Wang D-Y, Aballay A (2015) Genetic screen reveals link between maternal-effect sterile gene *mes-1* and *P. aeruginosa*-induced neurodegeneration in *C. elegans*. J Biol Chem 290:29231–29239
44. Yu Y-L, Zhi L-T, Guan X-M, Wang D-Y, Wang D-Y (2016) FLP-4 neuropeptide and its receptor in a neuronal circuit regulate preference choice through functions of ASH-2 trithorax complex in *Caenorhabditis elegans*. Sci Rep 6:21485
45. Sun L-M, Zhi L-T, Shakoor S, Liao K, Wang D-Y (2016) microRNAs involved in the control of innate immunity in *Candida* infected *Caenorhabditis elegans*. Sci Rep 6:36036
46. Sun L-M, Liao K, Li Y-P, Zhao L, Liang S, Guo D, Hu J, Wang D-Y (2016) Synergy between PVP-coated silver nanoparticles and azole antifungal against drug-resistant *Candida albicans*. J Nanosci Nanotechnol 16:2325–2335
47. Sun L-M, Liao K, Hong C-C, Wang D-Y (2017) Honokiol induces reactive oxygen species-mediated apoptosis in *Candida albicans* through mitochondrial dysfunction. PLoS ONE. 2017 12:e0172228

48. Sun L-M, Liao K, Wang D-Y (2017) Honokiol induces superoxide production by targeting mitochondrial respiratory chain complex I in *Candida albicans*. PLoS ONE 12:e0184003
49. Zhi L-T, Yu Y-L, Li X-Y, Wang D-Y, Wang D-Y (2017) Molecular control of innate immune response to *Pseudomonas aeruginosa* infection by intestinal *let-7* in *Caenorhabditis elegans*. PLoS Pathog 13:e1006152
50. Yu Y-L, Zhi L-T, Wu Q-L, Jiang L-N, Wang D-Y (2018) NPR-9 regulates innate immune response in *Caenorhabditis elegans* by antagonizing activity of AIB interneurons. Cell Mol Immunol 15:27–37
51. Zhi L-T, Yu Y-L, Jiang Z-X, Wang D-Y (2017) *mir-355* functions as an important link between p38 MAPK signaling and insulin signaling in the regulation of innate immunity. Sci Rep 7:14560
52. Garcia SMDA, Tabach Y, Lourenço GF, Armakola M, Ruvkun G (2014) Identification of genes in toxicity pathways of trinucleotide-repeat RNA in *C. elegans*. Nat Struct Mol Biol 21:712–720